

1 **A predictive model for Lake Chad total surface water area using remotely sensed and**  
2 **modeled hydrological and meteorological parameters and multivariate regression analysis**

3

4 **Frederick Policelli <sup>a,d</sup>, Alfred Hubbard <sup>b,c</sup>, Hahn Chul Jung <sup>a,c</sup>, Ben Zaitchik <sup>d</sup>, Charles**  
5 **Ichoku <sup>e</sup>**

6 <sup>a</sup> NASA Goddard Space Flight Center

7 8800 Greenbelt Rd

8 Code 617, Hydrological Sciences Lab

9 Greenbelt, MD, 20771, USA

10

11 <sup>b</sup> NASA Goddard Space Flight Center

12 8800 Greenbelt Rd

13 Code 618, Biospheric Sciences Lab

14 Greenbelt, MD, 20771, USA

15

16 <sup>c</sup> Science Systems and Applications, Inc.

17 10210 Greenbelt Rd

18 Lanham, MD, 20706, USA

19

20 <sup>d</sup> Johns Hopkins University

21 Dept. of Earth and Planetary Sciences

22 3400 N. Charles St.

23 Baltimore, MD 21218, USA

24

25 <sup>e</sup> Howard University

26 Dept. of Interdisciplinary Studies

27 1840 7th Street, NW

28 Washington, DC 20001, USA

29

30 \* Correspondence: [frederick.s.policelli@nasa.gov](mailto:frederick.s.policelli@nasa.gov); Tel.: +01-301-614-6573

31

32

33

34

35

36

37

38

39 **Abstract**

40 Lake Chad is an endorheic lake in west-central Africa at the southern edge of the Sahara  
41 Desert. The lake, which is well known for its dramatic decrease in surface area during the 1970s  
42 and 1980s, experiences an annual flood resulting in a maximum total surface water area  
43 generally during February or March, though sometimes earlier or later. People along the shores  
44 of Lake Chad make their living fishing, farming, and raising livestock and have a vested interest  
45 in knowing when and how extensive the annual flooding will be, particularly those practicing  
46 recession farming in which the fertile ground of previously flooded area is used for planting  
47 crops. In this study, the authors investigate the relationship between lake and basin parameters,  
48 including rainfall, basin evapotranspiration, lake evapotranspiration, lake elevation, total surface  
49 water area, and the previous year's total surface water area, and develop equations for each dry  
50 season month (except November) linking total surface water area to the other parameters. The  
51 resulting equations allow the user to estimate the December average monthly total surface water  
52 area of the lake in late November, and to make the estimates for January to May in early  
53 December. Based on the results of a Leave One Out Cross Validation analysis, the equations for  
54 lake area are estimated to have an average absolute error ranging from 5.3 percent (for February  
55 estimates) to 7.6 percent (for May estimates).

56

57 <sup>1</sup>Keywords: surface water area, Lake Chad, precipitation, evapotranspiration, lake height

## 58 **1. Introduction**

59 Lake Chad is a shallow, endorheic lake in the Sahel region of west-central Africa shared by  
60 Chad, Nigeria, Niger, and Cameroon. There have been numerous hydrological models  
61 developed for Lake Chad. Each of these has limitations relative to the statistical model for lake  
62 area we present here.

63 Bader et al. (2011) developed a hydrological model that simulates the water level in the  
64 northern pool, southern pool, and archipelago using riverine and direct rainfall inputs to the lake.  
65 It also estimates total water area for each of the pools. According to (Lemoalle et al., 2012), the  
66 model results correspond well with satellite measurements of northern pool surface water area  
67 and with satellite measurements of the total surface water area from 1980 onward, though these

---

Abbreviations: Inter-Tropical Convergence Zone (ITCZ), above sea level (ASL), Climate Hazards  
Group InfraRed Precipitation with Station data (CHIRPS), Famine Early Warning Systems Network  
(FEWS NET) Land Data Assimilation System (FLDAS), Land Surface Temperature (LST),  
evapotranspiration (ET), Leave One Out Cross Validation (LOOCV), precipitation (P). For reading  
regression results: Pws is total south basin wet season precipitation, ETws is total south basin wet season  
evapotranspiration, LakeETws is wet season lake ET percent variation from the 1988 to 2016 wet season  
mean, H is November lake height variation from the 1993-2002 mean, A is the average surface water area  
for the given month, A- is the previous year's average surface water area for the given month.

68 results are not quantified. One disadvantage of this model is that it requires input of the Chari  
69 River and Komodougu-Yobe River discharges, data that is not publicly available.

70 Coe and Foley (2001) report the results of a hydrological model of Lake Chad. They describe  
71 a model with “good agreement with the inferred lake area” during simulations for the years 1954  
72 to 1967. The “inferred lake area” is not a direct measurement of lake area, but rather is derived  
73 from a relationship between lake area and lake level. It is important to note that the hydrology of  
74 Lake Chad changed significantly in the 1970’s during its transition from “Normal Lake Chad” to  
75 “Small Lake Chad” and the model, based on a coarse (10 km resolution) digital elevation model,  
76 may not be adequate to define the lake after this transition.

77 Gao et al. (2011) developed a hydrological model of Lake Chad. They compared images of the  
78 lake extent from the model with images derived from remote sensing. Three image pairs were  
79 shown, for October 31, 1963; December 25, 1972; and January 31, 1987. Each pair of images  
80 from the two earlier dates (before the transition from “Normal Lake Chad” to “Small  
81 Lake Chad”) looked quite similar, though no numerical value was provided. The model-  
82 observation pair for the post transition period did not look very similar. This raises the question  
83 of the utility of the model for producing lake area in the current, post transition period.

84 Lemoalle (2004) developed a crude expression for Lake Chad surface area based on a  
85 simplified water balance model and described it as a “first approximation.” That model assumes  
86 no seepage from the lake and requires knowledge of the streamflow to the lake, which as  
87 previously noted is not publicly available. Delclaux et al. (2008) developed a hydrological

88 model of the Lake Chad Basin, however the results they presented included streamflow and  
89 elevation, but not surface area.

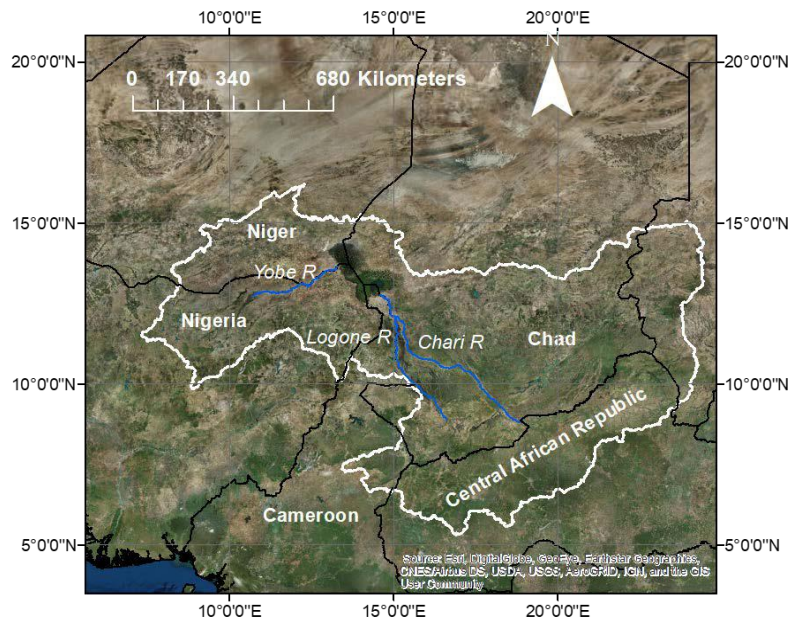
90 Coe and Birkett (2004) used upstream measurement of river height along with in-situ stream  
91 flow and gauge height to estimate river discharge 500 km downstream and wet season height of  
92 Lake Chad, greater than 600 km downstream. Their method, though, clearly relies on hard-to-  
93 obtain in-situ measurements and does not include lake area.

94 The first objective of this paper is to assemble and examine a set of satellite- and model-based  
95 data for the southern Lake Chad Basin relevant to developing a statistical model for the area of  
96 the lake during its flooding season. This data set includes time series of satellite- and gauge-  
97 based precipitation and modeled ET for the southern part of the basin, modeled lake ET data,  
98 satellite-based lake elevation data, and satellite-based estimated lake total surface water area.  
99 Given the limitations of the existing models described above, the second objective is to develop a  
100 predictive statistical model for total lake surface water area using regression methods on the data  
101 set. The regression method includes backward elimination variable selection and a Leave One  
102 Out Cross Validation (LOOCV) analysis to optimize the resulting statistical model.

## 103 **2 Study Area**

104 The Lake Chad basin is approximately 2.5 million square kilometers, about eight percent of  
105 the African continent, and the largest endorheic basin in the world (Gao et al., 2011). Lake Chad  
106 is the terminal lake of this basin. The northern part of the basin lies within the Sahara and does  
107 not generate runoff that reaches Lake Chad (Delclaux et al., 2008).

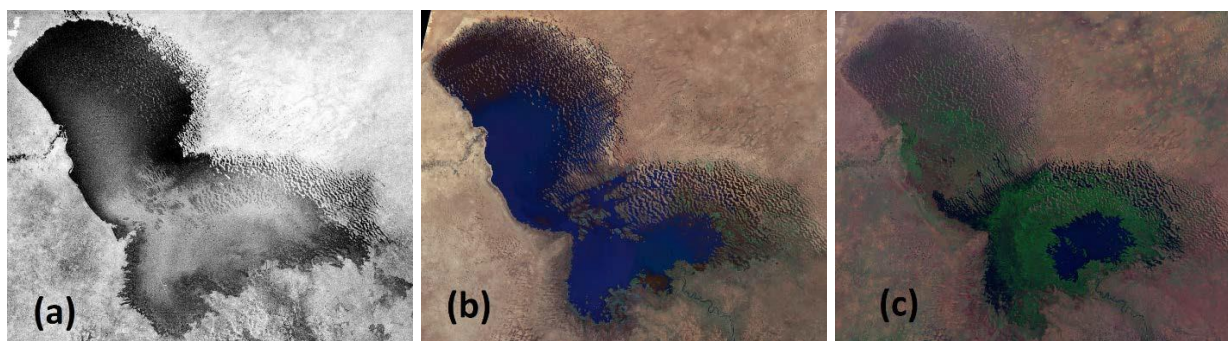
108 For this reason, we work with the southern part of the basin (figure 1).

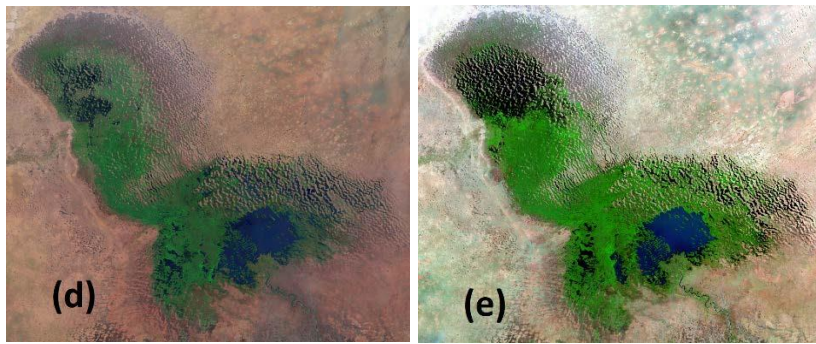


109 Fig. 1 Southern Lake Chad Basin (white), lake, and major rivers (blue)

110 The lake's average depth varies between 1.5 and 5 m. Any change in lake volume translates to a  
111 substantial change in lake shoreline and area ("Lake Chad flooded savanna", World Wildlife  
112 Fund, no date, <https://www.worldwildlife.org/ecoregions/at0904>).

113 In the 1960's the lake's area was on the order of 25,000 sq. km.; in the mid-1980s its area was  
114 reported to be about one tenth of that size (Grove, 1996), though it is not clear if that includes  
115 flooded vegetation. If one includes flooded vegetation, the lake's annual peak area for 2017 is  
116 estimated at close to 14,700 sq. km (Policelli et al., 2018). Figure 2 shows the evolution of Lake  
117 Chad from the time of the earliest space-based images of the lake.





118 Fig. 2 Evolution of Lake Chad. Optical imagery from (a) 1963, Argon satellite (b) 1973,  
119 Landsat 1 (c) 1987, Landsat 5 (d) 2003, Landsat 7 (e) 2013, Landsat 8. Images provided by U.S.  
120 Geological Survey, Department of the Interior/USGS

121

122 Below about 280 m ASL, the lake separates into a southern pool and a northern pool divided by  
123 “the Great Barrier”, and the southern pool separates from the eastern “archipelago” of sandy  
124 islands (Lemoalle, 2004).

125 The population of the lake shore is around 2 million (Magrin, 2016) and the people make a  
126 living through a combination of fishing, farming, and raising livestock (Sarch and Birkett, 2000).  
127 “Recession farming” is an important method of farming in the region whereby farmers plant in  
128 the enriched soils following each year’s flood pulse. Because of the complexity of the  
129 hydrology, it is difficult to provide farmers with information on the timing of the floods and a  
130 sense of how large the flood is going to be in any given year. This can be a serious problem for  
131 farmers who grow crops near the lake shore and periodically lose crops to flooding (Okpara et



132 al., 2016).

133 According to (Sarch and Birkett, 2000), the “farming start date” at villages on the south-west  
134 shore of Lake Chad begins in mid-January to late February. It seems reasonable to conclude that  
135 predictions of lake surface area made in late November or early December could be used for  
136 agricultural decision making for locations with similar start dates.

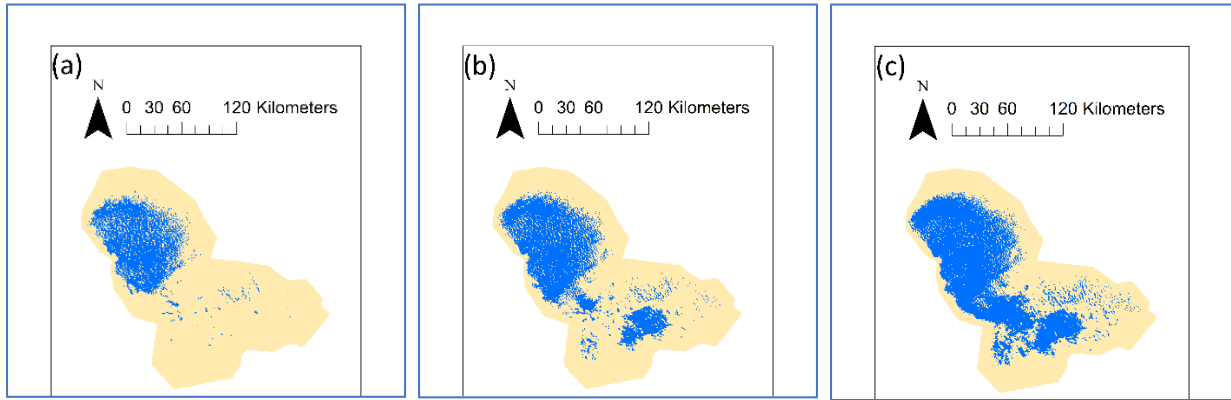
137 There are a number of dams and irrigation schemes in the river basins that drain into Lake  
138 Chad, such as those of the Chari-Logone and Komadougou-Yobe river systems. However, at the  
139 large scale, they do not amount to a substantial revision of the natural seasonal hydrological  
140 patterns, which are largely determined by the West African Monsoon and the position of the  
141 ITCZ (Birkett, 2000).

142 The surface of Lake Chad is not flat and level; the barriers to flow from the southern pool to  
143 the northern pool and archipelago result in the water in these areas frequently being at different  
144 elevations. Additionally, the local winds and flow of water from the Chari River into the lake  
145 (addressed further in the Discussion section) combined with the complex shape of the lake lead  
146 to an evolving lake surface (Carmouze et al., 1983). Lake surface elevation time series data used  
147 in this study refer to satellite-based measurements made in the relatively small open water  
148 portion of the lake in the southern pool.

149 Figure 3 presents areas of the lake at or below selected elevations. The topographic data used  
150 to create figure 3 is from a 1 arc-second (~30m) resolution Digital Elevation Model (DEM) from  
151 the NASA Shuttle Radar Topography Mission (SRTM). The blue areas would correspond to lake  
152 levels (limited by the accuracy of the DEM) if the lake surface were flat and the lake filled

153 uniformly. However, since this is not the case, the areas should only be viewed as providing  
154 context for Lake Chad landforms and hydrology.

155



156 Fig. 3 Blue areas have elevations at or below (a) 279m ASL, (b) 280m ASL, (c) 281m ASL

157

158 According to (Leblanc et al., 2011) most of the flooded area of Lake Chad is covered by  
159 aquatic vegetation including rooted and floating plants. This area is not readily measured with  
160 optical remote sensing, but must be accounted for to get an accurate estimate of total surface  
161 water area for the lake (Policelli et al., 2018).

162 Lake Chad receives 90-96% of its water from the Chari-Logone River system (Zhu et al.,  
163 2017a), with the remaining coming from smaller tributaries and direct rainfall. Most of this  
164 water arrives from such a distance that the peak lake level and lake area occur months after the  
165 rainfalls that produce them. The delay is due to the slow runoff and routing of flood water to  
166 Lake Chad from the southern portion of the basin where precipitation rates are highest (Leblanc  
167 et al., 2011). It is the reason that the Lake Chad peak level and area take place in the dry season.

## 168 **3 Data and Methods**

### 169 **3.1 Data**

170 The key datasets used for this research are (1) Climate Hazards Group Infrared Precipitation  
171 with Station data (CHIRPS), (2) satellite altimetry-based lake surface elevation data, (3)  
172 evapotranspiration (ET) data from the Famine Early Warning Systems Network (FEWS NET)  
173 Land Data Assimilation System (FLDAS), (4) percent of 1988-2016 lake ET average estimates,  
174 (5) the HydroBASINS shape file for the southern Lake Chad Basin extent and (6) lake total  
175 surface water area data, described in (Policelli et al., 2018).

176 **3.1.1** CHIRPS (Funk et al., 2015) is a quasi-global precipitation dataset produced by the Climate  
177 Hazards Group at the University of California, Santa Barbara using both satellite data and rain  
178 gauge data. We used the high resolution (.05 degree x .05 degree) daily Africa rainfall dataset,  
179 which is available from January, 1981 and updated through the previous month around the third  
180 week of each month. In comparison with the lower resolution gauge-based GPCC reference  
181 precipitation product (Schneider et al., 2015), for wet seasons in Africa CHIRPS has a mean error  
182 of 79 mm per 3 months, a mean bias of 0.22 and a correlation of 0.56 (Funk et al., 2015). In  
183 comparison with other observations-based precipitation products for Africa, CHIRPS data has  
184 higher spatial resolution, better coverage of rain gauge stations, and applies improved statistical  
185 methods (Badr et al., 2016).

186 **3.1.2** Lake surface elevation data are provided by the Global Reservoir and Lake Monitor (G-  
187 REALM) on the USDA Crop Explorer website (“Satellite Radar Altimetry: Global Reservoir and  
188 Lake Elevation Database,” no date,

189 [https://www.pecad.fas.usda.gov/cropexplorer/global\\_reservoir/](https://www.pecad.fas.usda.gov/cropexplorer/global_reservoir/)). Lake surface elevation data are  
190 produced from the radar altimetry satellite missions Topex/Poseidon (1992-2002), Jason-1  
191 (2002-2008), Jason-2 (2008 to 2016), and Jason-3 (2016 to present). The altimeters have a  
192 “footprint” diameter ranging from about 200m to several kilometers depending on the target’s  
193 surface roughness. Each of the altimeters used for Lake Chad elevation data have a ten-day  
194 repeat time. The accuracy of the lake surface elevation data for Lake Chad is approximately 0.29  
195 m (Ricko et al., 2012). Lake surface elevation data are provided as the variation from the 1993-  
196 2002 mean height.

197 **3.1.3** The FLDAS ET data product is based on the Noah 3.3 Land Surface Model’s total ET,  
198 which is the sum of bare soil evaporation, evaporation of water intercepted by the canopy, and  
199 transpiration, weighted by the coverage fraction of each component (McNally et al., 2017). The  
200 spatial resolution of the FLDAS ET is 0.1 degree and we are using monthly data. The FLDAS  
201 ET data is available from October 1992 to the present. FLDAS ET has been evaluated against  
202 estimates from the Simplified Surface Energy Balance (SSEBop) satellite data-based model  
203 (Senay et al., 2013). This evaluation indicates that FLDAS and SSEBop ET have significant but  
204 limited correlation ( $r < 0.5$ ) for percentage ET variations in West Africa. According to McNally  
205 et al., 2017, it is not entirely clear why the correlation between the FLDAS-ET and SSEBop-ET  
206 is somewhat poor in West Africa, though it may have something to do with instability of the  
207 SSEBop algorithm in that area.

208 **3.1.4** We estimated the Lake Chad wet season ET as a percentage of the 1988-2016 wet season  
209 average. Because most (approximately constant at nearly 90 percent by our estimation) of the

210 lake consists of flooded vegetation, and multiple types of vegetation are present, it is a very  
211 difficult research problem to estimate the total monthly ET from Lake Chad. However, because  
212 the ratio of open water to flooded vegetation is roughly constant over time, we were able to  
213 estimate the lake ET percent of average as the ratio of the open water evaporation for the full  
214 extent of the lake to the average open water evaporation for the full extent of the lake for 1988-  
215 2016. We used the Complementary Relationship Lake Evaporation (CRLE) model (Morton,  
216 1986) for estimates of lake open water evaporation. The meteorological forcing data for the  
217 CRLE model were provided by NOAA NCEP-DOE Reanalysis 2. The main validation work by  
218 the developers of the CRLE model was to compare model results with lake evaporation from  
219 water balance analyses for seventeen selected lakes. On an annual basis, the model results were  
220 within a maximum of seven percent of the water balance results. Monthly results suffered an  
221 unspecified degradation of accuracy (Morton, 1986).

222 **3.1.5** The World Wildlife Fund (WWF) HydroBASINS (Lehner, 2013) provided the shape file  
223 for the southern Lake Chad Basin, which was used to calculate rainfall and ET for the portion of  
224 the basin that generates very nearly all of the runoff that reaches the lake. The HydroBASINS  
225 global database of basin shapes was developed using the WWF HydroSHEDS data (Lehner et  
226 al., 2011), which has approximately 500 m resolution. The HydroSHEDS product was  
227 developed using SRTM data. No validation description or accuracy assessment was found for  
228 HydroBASINS.

229 **3.1.6** Lake Chad total surface water area data from the research for (Policelli et al., 2018) were  
230 derived from (1) 1 km resolution Land Surface Temperature (LST) data from the NASA Terra

231 satellite's MODIS sensor and adjusted using ESA C-band radar data from Sentinel-1a, and (2)  
232 total Lake Chad surface water area estimates by (Leblanc et al., 2011) derived from 5 km  
233 resolution LST data from the Meteosat MVIRI sensor and bias corrected by (Policelli et al.,  
234 2018). The LST method for estimating lake surface water area is based on the fact that the lake,  
235 including flooded vegetation, is cooler than the surrounding landscape during the day (Leblanc et  
236 al., 2011). Monthly average area was used for this research. This data was produced for the  
237 1988-1989 dry season through the 2016-2017 dry season. MODIS LST data with cloud cover  
238 greater than five percent were not used in the development of the lake area data. The validation  
239 done for this data was comparison of the two datasets used to create the lake area time series.  
240 The estimated lake areas for the two products during the period of overlap were within  
241 approximately three percent of each other.

### 242 **3.2 Methods**

243 Monthly precipitation and ET were calculated for the southern portion of the basin from  
244 October 1992 to May 2017 using the HydroBASINS shape file for this area. The Lake Chad  
245 total surface water area time series was then checked for correlation with P-ET using a series of  
246 time lags to find the peak correlation. It was expected that net precipitation (P-ET) would be  
247 more closely correlated to lake area than either of the components. Similarly, the total lake  
248 surface water area was checked for correlation with the lake elevation data, and it was expected  
249 that a close correlation would exist between these variables (Busker et al., 2018). Additionally,  
250 the total lake surface water area was checked for correlation with the lake elevation data, the

251 precipitation data and the ET data for the southern portion of the basin, the lake ET percentage of  
252 1988-2016 average lake ET, and the previous year's total lake surface water area.

253 Next, a multivariate regression analysis was performed using the datasets to establish  
254 equations linking total surface water area for a given month to one or more of the other  
255 (independent) variables. In order to find the best relationship between the lake area and the  
256 independent variables, we used several methods of regression: 1<sup>st</sup> order linear regression, 2<sup>nd</sup>  
257 and 3<sup>rd</sup> order polynomial regression, and the linear-log method of regression. We also used the  
258 backward elimination method of variable selection to optimize the equations. To mitigate the  
259 risk of overfitting the data, we used the "rule of thumb" of ten data points for each variable  
260 included in the final equation (Harrell et al., 1996), except for 1<sup>st</sup> order linear regression, in  
261 which case as few as two data points for each variable included is permitted (Austin and  
262 Steyerberg, 2015). However, we did not use less than six data points for each variable in our 1<sup>st</sup>  
263 order linear regression analysis.

264 The current year's total surface water area for each month during the dry season was the  
265 dependent variable. The independent variables were (1) total wet season precipitation for the  
266 southern Lake Chad Basin, (2) total wet season ET for the southern Lake Chad Basin, (3) wet  
267 season lake ET as a percentage of the 1988-2016 average lake ET, (4) November (typically the  
268 highest) variation from the 1993-2002 mean lake surface height, and (5) the total surface water  
269 area of the given month for the previous year. A Leave One Out Cross Validation (LOOCV) was  
270 performed for the regression analysis, in which one data point was left out, the equation was

271 generated using regression, and the equation was evaluated for the one left out data point. This  
272 was repeated for each yearly data point and an average absolute value of the percent error was  
273 determined for the total dataset. For comparison, the average absolute value of the percent error  
274 was also determined using the average total surface water area for a given month as the  
275 prediction, and using the previous year's area as the prediction for a given month.

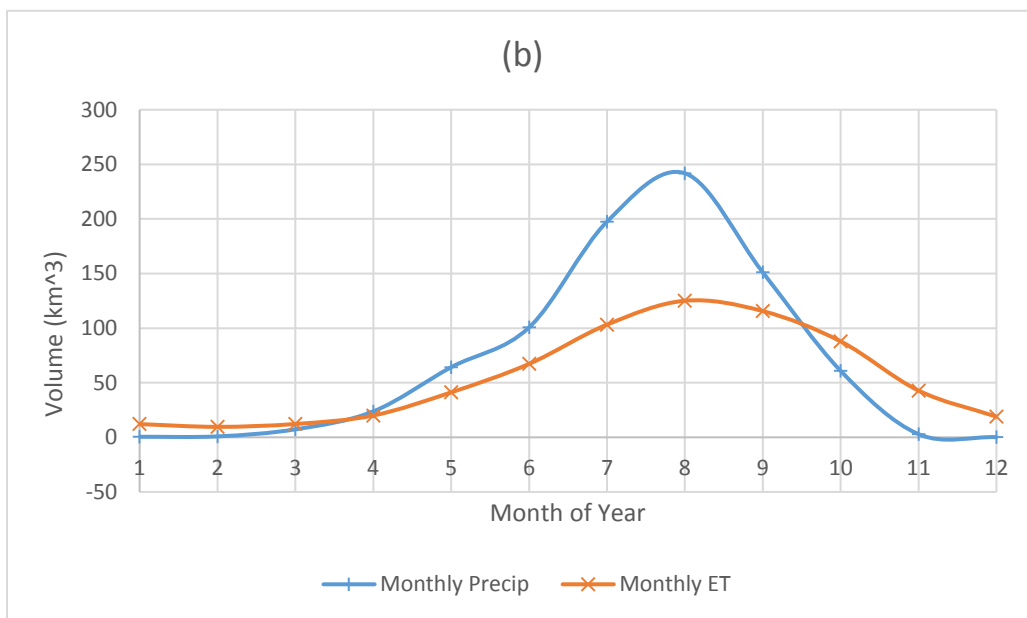
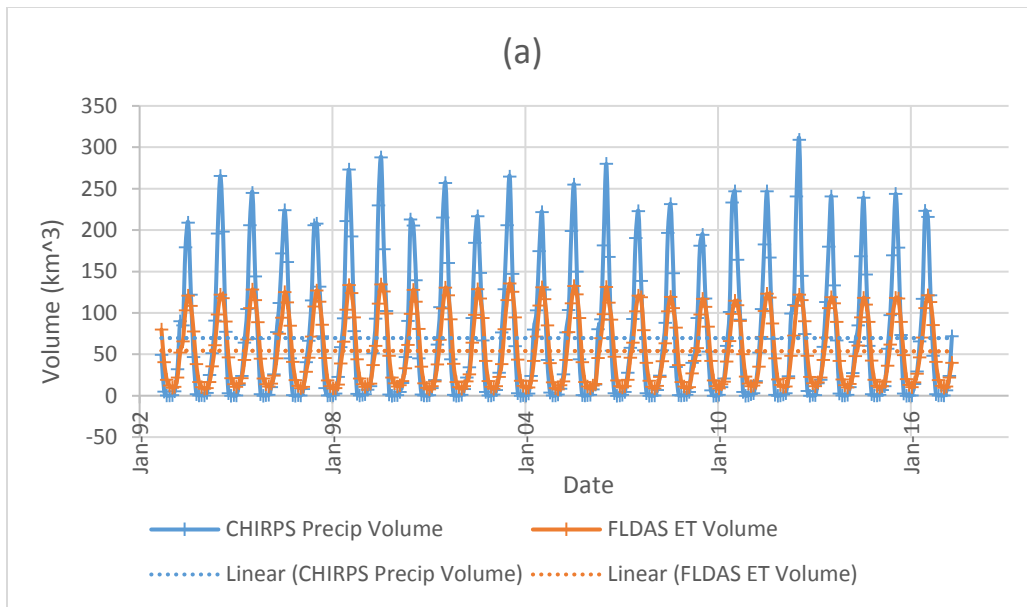
276 The study covered the time period from October 1992 to May 2017 which is the intersection  
277 of the period of available FLDAS evapotranspiration data and the available total lake surface  
278 water area data. Three years (2006-2008) were excluded from the study because of insufficient  
279 lake surface elevation data.

## 280 **4. Results**

### 281 **4.1 Datasets**

282 Total monthly precipitation and ET for the southern portion of the Lake Chad Basin were  
283 calculated using CHIRPS and FLDAS, respectively. Figure 4.a. shows the total monthly  
284 precipitation and ET for October 1992 through May 2017. The trend lines indicate essentially no  
285 change over this time period. Figure 4.b. shows the average monthly distribution of the  
286 precipitation and ET for the southern portion of the basin for October 1992 through May  
287 2017. June through October is usually considered the wet season and November through May is  
288 considered the dry season (figure 4.b and Leblanc et al., 2011).



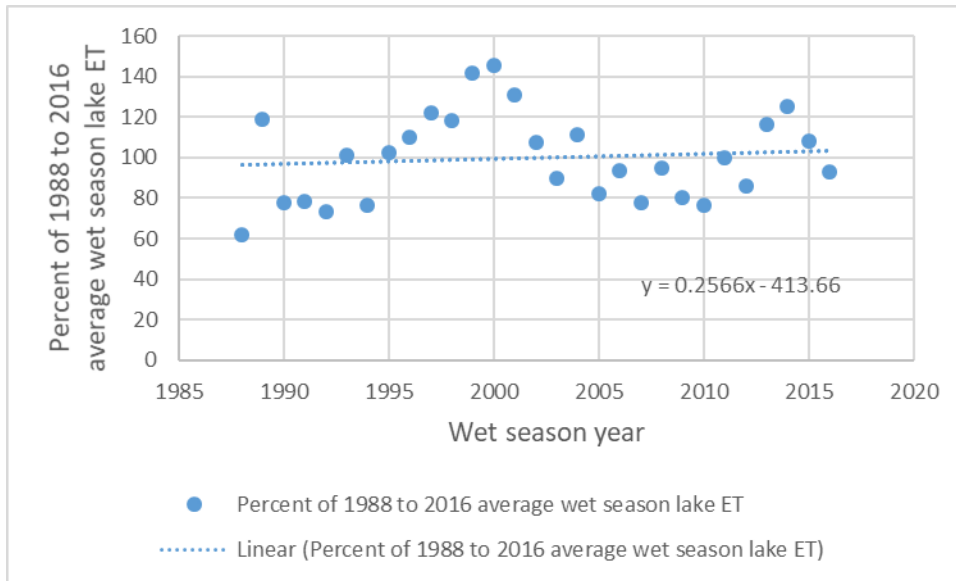


289 Fig. 4 a. monthly precipitation and ET in the Southern portion of the Lake  
 290 Chad Basin b. average monthly precipitation and ET in the Southern portion of the  
 291 Lake Chad Basin

292

293 Figure 5 shows the percent of Lake Chad wet season average ET from 1988 to 2016. The

294 data exhibits an oscillatory behavior with a multi-year cycle and the trend is essentially flat.



295

296 Fig. 5 Percentage of 1988 to 2016 average wet season lake ET

297

298 Figure 6.a. shows the lake elevation anomaly relative to the 1993-2002 mean level for

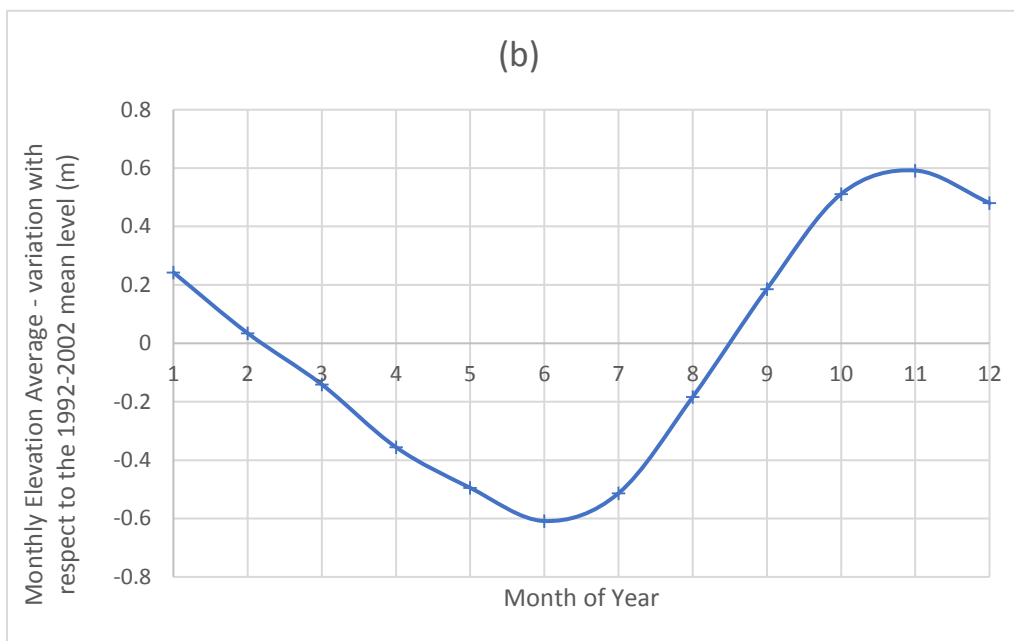
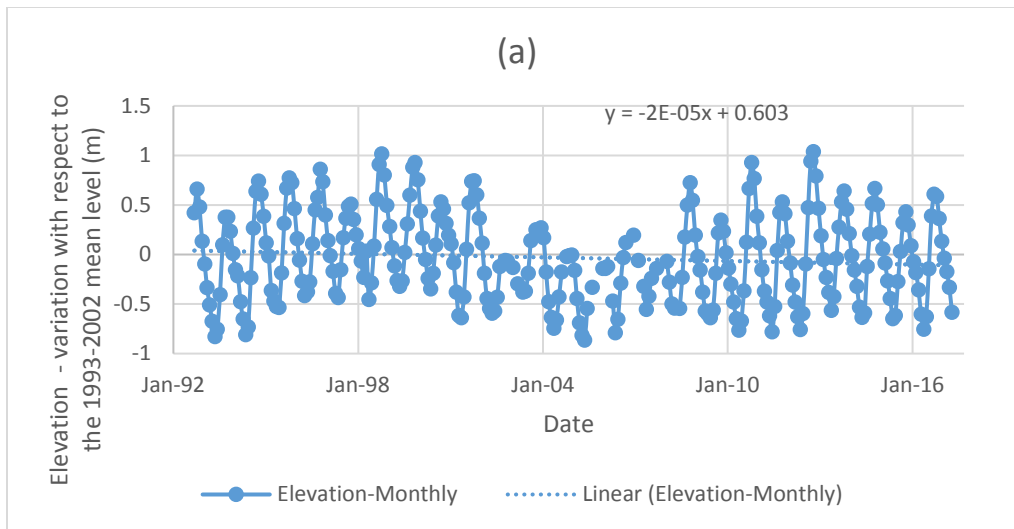
299 October 1992 to May 2017. The trend line for July (the only month with complete data; not

300 shown) shows a slight level of decrease with high variability. Figure 6.b. shows the average

301 monthly lake elevation anomalies with respect to the 1993-2002 mean level for October 1992

302 through May 2017. Note that the average level is highest in November (during the dry season)

303 and lowest in June (during the wet season).



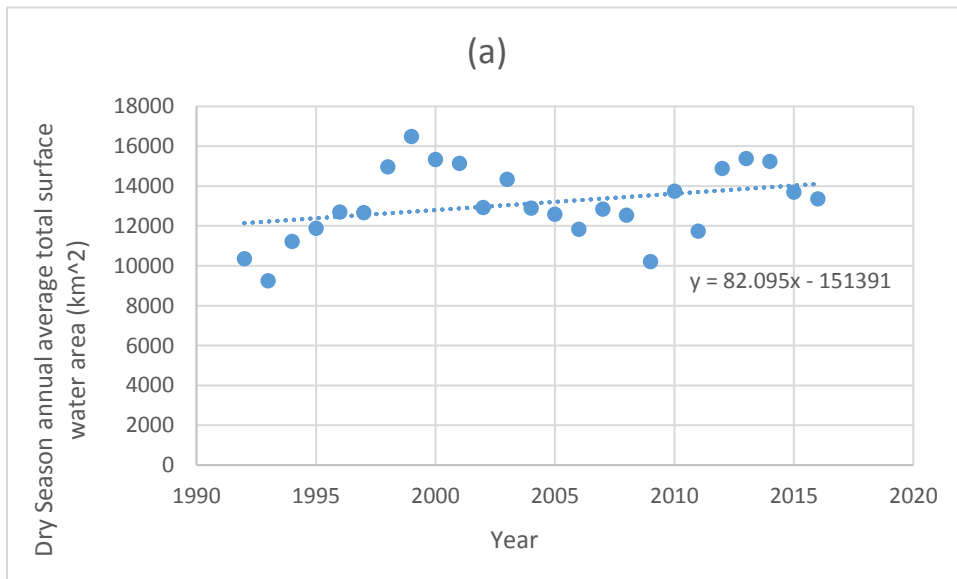
304 Fig. 6 a. lake elevation anomaly relative to the 1993-2002 mean level

305 b. average monthly lake elevation anomaly relative to the 1993-2002 mean level

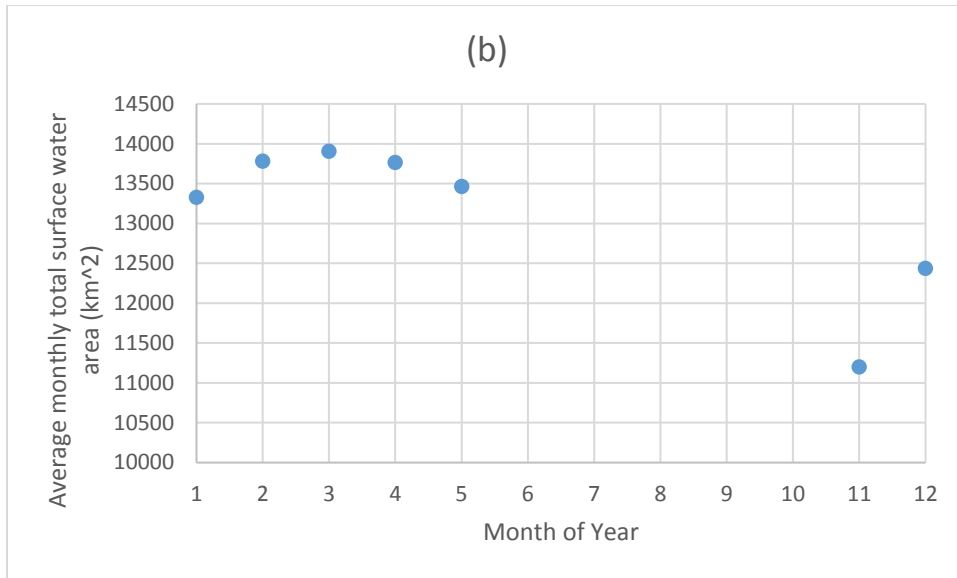
306

307 Figure 7.a. presents the annual average dry season surface water area for Lake Chad from

308 November 1992 through May 2017. As expected, the pattern of the graph is similar to that of the  
309 graph of Lake Chad percentage of 1988 to 2016 average wet season lake ET (figure 5). The  
310 trend line shows an average increase of approximately 82 square kilometers per year in lake area  
311 over this period. Wet season data was not considered suitable for calculation of water extent  
312 because of cloud coverage and the fact that the LST method cannot distinguish well between soil  
313 moisture and flooded areas (Policelli et al., 2018). The total surface water area includes both  
314 open water and flooded vegetation. Figure 7.b. presents the average dry season monthly total  
315 surface water area for Lake Chad from November 1992 through May 2017. While the peak  
316 water elevation occurs on average in November, the peak total surface water area occurs in  
317 March on average. The peak total surface water area is not a sharp peak; the two antecedent and  
318 two following months are not far from the maximum



319



320 Fig. 7 a. average annual dry season water extent for Lake Chad b. average monthly  
 321 lake water area for the dry season (November 1992 through May 2017)

322

#### 323 4.2 A predictive model for Lake Chad total surface water area

324 During this part of the research, we asked the question: “for a given month, how well can we  
 325 predict the total surface water area of Lake Chad”? To address this question, we investigated  
 326 regression of the data to generate equations linking the independent variables to the dependent  
 327 variable. Specifically, we looked at 1<sup>st</sup> order linear equations (Equation 1), 2<sup>nd</sup> order  
 328 polynomial equations (Equation 2), 3<sup>rd</sup> order polynomial equations (Equation 3), and linear-log  
 329 equations (Equation 4).

330 Equation 1:  $A = a + b \cdot ETws + c \cdot LakeETws + d \cdot Pws + e \cdot H + f \cdot A-$

331 Equation 2:  $A = a + b \cdot ETws + c \cdot ETws^2 + d \cdot LakeETws + e \cdot LakeETws^2 + f \cdot Pws +$

332 
$$g \cdot Pws^2 + h \cdot H + j \cdot H^2 + k \cdot A^- + m \cdot A^{-2}$$

333 Equation 3: 
$$A = a + b \cdot ETws + c \cdot ETws^2 + d \cdot ETws^3 + e \cdot LakeETws + f \cdot LakeETws^2$$

334 
$$+ g \cdot LakeETws^3 + h \cdot Pws + j \cdot Pws^2 + k \cdot Pws^3 + m \cdot H + n \cdot H^2 + p \cdot H^3 +$$

335 
$$q \cdot A^- + r \cdot A^{-2} + s \cdot A^{-3}$$

336 Equation 4: 
$$A = a + b \cdot \log(ETws) + c \cdot \log(LakeETws) + d \cdot \log(Pws) + e \cdot \log(H) +$$

337 
$$f \cdot \log(A^-)$$

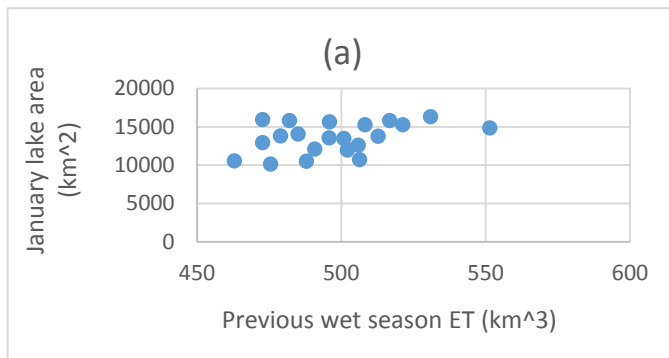
338 where:  $A = A_{Lake\ Chad, t}$  ,  $ETws = \sum_{June}^{Oct.} basin\ ET$  ,  $LakeETws = \sum_{June}^{Oct.} lake\ E / lake\ E_{1988-2016\ avg}$ ,

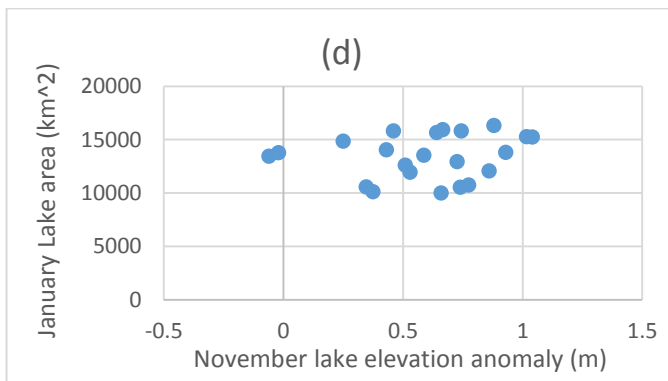
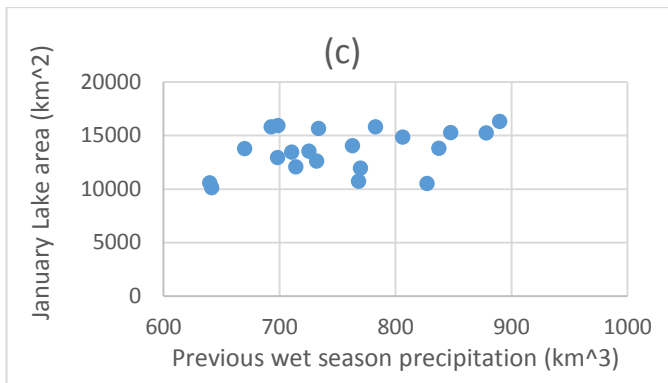
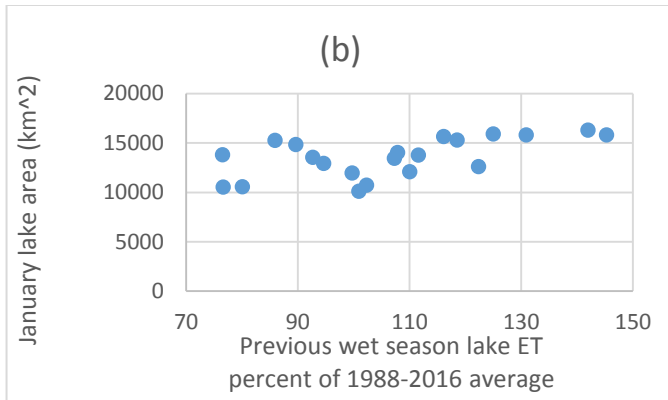
339  $Pws = \sum_{June}^{Oct.} basin\ P$  ,  $H = Lake\ Elevation_{Nov} - Lake\ Elevation_{1993-2002\ avg}$  , and

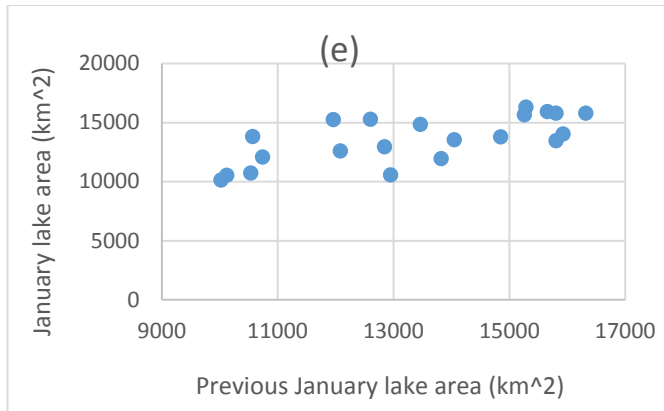
340  $A^- = A_{Lake\ Chad, t-1\ year}$

341 Figure 8 shows the scatter plots for each of the independent variables versus the average lake

342 area for January.







343 Fig. 8 Example (January) scatter plots for independent variables vs. lake area (a) previous wet  
 344 season ET, (b) previous wet season lake ET percentage of the 1988-2016 average, (c) previous  
 345 wet season precipitation, (d) November lake elevation anomaly, (e) previous January lake area.  
 346

347 From our regression analysis we found that for the equation types we examined, 1<sup>st</sup> order linear  
 348 equations provided the minimum average absolute percent error from LOOCV for December,  
 349 February and May. For January, March and April, higher order polynomial equations provided  
 350 slightly lower (between 0.7% and 1.1% lower) LOOCV average absolute percent errors.

351 However, because of the lack of a physical explanation for some of the higher order terms ( $A^{-2}$   
 352 and  $A^{-3}$  for instance), and the marginal gain for using the higher order equations, we decided to  
 353 maintain consistency across months and use optimized 1<sup>st</sup> order linear equations for all months.  
 354 Linear-log solutions for the regression analysis provided higher LOOCV average absolute  
 355 percent errors than the linear 1<sup>st</sup> order and polynomial solutions. The final equations are  
 356 provided in Table 1.



357

358 Table 1 Equations and performance metrics for Lake Chad total surface water estimated area in

359 terms of ETws, LakeETws, Pws, H, A-

Forecast Mo.	Lake Area Equation	LOOCV error (%)	LOOCV std (%)	Adjusted R-Squared
December	$-7064.38 + 23.53 * \text{LakeETws} + 12.57 * \text{Pws} + 0.62 * \text{A}$	6.05	4.60	0.78
January	$-11641.42 + 25.59 * \text{ETws} + 3364.12 * \text{H} + 0.78 * \text{A}$	6.90	4.91	0.76
February	$-8443.93 + 14.40 * \text{Pws} + 1771.05 * \text{H} + 0.76 * \text{A}$	5.25	4.66	0.80
March	$-7042.42 + 14.36 * \text{Pws} + 2074.06 * \text{H} + 0.65 * \text{A}$	7.20	5.95	0.69
April	$-5187.30 + 12.75 * \text{Pws} + 2249.73 * \text{H} + 0.59 * \text{A}$	7.53	5.14	0.64
May	$-7402.54 + 17.15 * \text{Pws} + 2203.80 * \text{H} + 0.50 * \text{A}$	7.61	6.03	0.70

360

361 The result is that this model, using three variables for each month, can be used in late

362 November (when the precipitation data is available) to predict the Lake Chad total surface water

363 area for December, and in early December, (when lake elevation data is available for November)

364 the model can be used to predict the total surface water area for January through May, with the

365 expectation of between 5.3 and 7.6 percent error on average. This compares with (Table 2) the

366 set of average absolute percent errors if the average value of the total water surface area for each

367 month is used as a prediction,

368

369 Table 2 Average absolute percent error with average value used as prediction.

	average absolute % error
December	14.1
January	13.8
February	13.0

March	12.4
April	11.8
May	13.1

370

371 and (Table 3) the set of average absolute percent errors if the previous year's total water surface  
 372 area for the given month is used as a prediction.

373

374

375

376

377

378

379 Table 3 Average absolute percent error with previous year's lake area used as prediction

	average absolute % error
December	10.0
January	9.0
February	10.6
March	12.5
April	12.8
May	15.6

380

381 For each of the months December through May, the regression approach provides a lower  
 382 average absolute percent error than either the average value used as a prediction, or the previous  
 383 year's area used as a prediction. As an example, for May, the LOOCV average absolute error is

384 7.6%, while the error using the average May area is 13.1% on average, and the error when using  
385 the previous year's area for May is 15.6% on average. Using the average May lake area of  
386 13,363 sq. km, these percentages are equivalent to 1017 sq. km, 1751 sq. km, and 2085 sq. km  
387 respectively.

## 388 **5. Discussion**

389 The lake elevation data show that the maximum average monthly elevation typically occurs in  
390 November (though on occasion in October, and once during our record in January). It is curious  
391 therefore that the maximum area typically though not always occurs in February or March. The  
392 reason for this seems to be the complex meteorology and hydrology of Lake Chad. The  
393 movement of the water in Lake Chad is influenced by both the winds and the Chari-Logone  
394 water supply. Monsoon winds drive the displacement of the southern waters toward the north,  
395 and movement begins around the northeastern end of the Great Barrier in June, at the end of the  
396 low water. The Chari-Logone flood waters begin in August and provide half of their water in  
397 October and November when the northeasterly wind known as the Harmattan drives the water  
398 back toward the southern pool. This is also when the satellite radar altimeters (which collect data  
399 over the southern pool) typically record the highest levels. During the peak of the riverine  
400 flooding, water again reaches the northern pool and also spreads into the archipelago from the  
401 south basin. Following the end of the movement of water to the north pool in January, there is a  
402 general spreading of water in the southern pool to the periphery until April. (Carmouze et al.,  
403 1983). These movements result in a complex and changing lake surface topography, and are  
404 likely the reason we find poor correlation between lake elevation and lake area.

405 A full parameterization of the Lake Chad system, as implemented by (Delclaux et al., 2008)  
406 using the GR\_B + THMB Model, includes precipitation and reference evapotranspiration as  
407 inputs, which are adjusted by a coefficient C, set such that the Nash coefficient is maximized for  
408 the monthly flows of the Chari-Logone River system. Precipitation is then split between a soil  
409 reservoir with maximum capacity A, and surface runoff, the amounts depending on the level of  
410 water in the soil reservoir. The soil reservoir drains through actual evapotranspiration and  
411 percolation, which generates sub-surface runoff. Elevation data from the Shuttle Radar  
412 Topography Mission (SRTM) are used for generating drainage directions and water  
413 accumulation areas. Two irrigation scenarios were modeled. Lake level data was used to  
414 validate the model results. In comparison, our model also uses precipitation and actual  
415 evapotranspiration as inputs, though only for the wet season. The timing of subsurface flow and  
416 surface flow through the river systems is simulated in our model by the delay between the wet  
417 season end and the month being forecast, and by the HydroBASINS shapefile for the southern  
418 Lake Chad Basin, which defines the limits of our representation of the lake watershed. Lake  
419 level is used in the GR\_B + THMB model as memory of previous conditions, whereas the lake  
420 area for the previous year is used in our model for this purpose. Unlike the GR\_B + THMB  
421 model, we do not model irrigation withdrawals; as discussed in the Introduction section, this is a  
422 small part of the overall hydrology of the Lake Chad Basin. While the GR\_B + THMB model  
423 uses stream flow data to calibrate the model, and lake elevation to validate the model, we use  
424 lake area estimates for these tasks and lake elevation as an additional input parameter.

425 The main limitation of the model we present here is that it is not a physically-based model and  
426 may not perform well for conditions outside of those in the database we have developed.  
427 For example, we are not able to do regressions and provide predictions for wet season months  
428 because we do not have surface water area data for those conditions (Policelli et al., 2018).  
429 Also, the performance may degrade if it is used outside of the range of areas for which the  
430 regression models were established (8,700 sq. km – 16,800 sq. km) or when the hydrology of the  
431 lake changes substantially, such as when “small Lake Chad” transitions to “normal Lake Chad”  
432 at about 18,000 sq. km. There is no fixed date at which the model becomes unusable. However,  
433 if it is used for operational forecasting, it would be wise to regularly update the model with new  
434 data as it becomes available.

## 435 **6. Conclusions**

436 We have built a record of remote sensing data and model products (precipitation,  
437 evapotranspiration, lake height, and lake area) for the Lake Chad Basin and used this record to  
438 run a correlation analysis and a regression analysis. From the correlation analysis (see  
439 Appendix), we have found (1) the highest correlation between basin evaporation and total lake  
440 surface water area is 0.43 and occurs with a seven month lag, (2) the highest correlation between  
441 lake height anomaly and total lake surface water area is 0.57 and occurs with a four month lag,  
442 (3) the highest correlation between precipitation and total lake surface water area is 0.39 and  
443 occurs with a seven month lag, (4) the highest correlation between percent of 1988-2016 average  
444 lake ET and the lake total surface water area is 0.65 at zero lag time, and (5) there is a correlation

445 of 0.63 between the surface water area and the previous year's surface water area for the same  
446 month.

447 Note that lake surface height is more closely correlated with total lake surface water area than  
448 is precipitation, as might be expected from a measurement further "downstream". Additionally,  
449 basin ET is closely correlated with basin precipitation as might be expected since the  
450 precipitation is the source water for ET. Finally, basin ET is slightly more closely correlated  
451 with total surface water area than basin precipitation.

452 From our regression analysis, we have derived a set of equations that can be used starting in  
453 late November for predicting the total surface water area of Lake Chad for a given month (except  
454 November) during the dry season. The best of these in terms of R-squared use all of our  
455 parameters: wet season precipitation (Pws), wet season south basin evapotranspiration (ETws),  
456 wet season lake evapotranspiration percent of 1988-2016 average (LakeETws), lake height  
457 variation relative to 2002-2009 (H), and the previous year's surface area for the given month (A),  
458 though we are likely overfitting the data when using all of these variables. The results of Leave  
459 One Out Cross Validation (LOOCV) testing and backward elimination variable selection show  
460 the best performing variables for December to be LakeETws, Pws and A-, for January they are  
461 ETws, H, and A-, and for February, March, April and May they are Pws, H, and A-. The  
462 regression equations perform at between 5.3 and 7.6 average absolute percent error in the  
463 LOOCV testing, and outperform predictions made using the average value for the given month or  
464 the previous year's total surface water area.

465 The predictions using all of the equations derived from regression in this study can be made  
466 with only remotely sensed data and model outputs; no in-situ data is required. Any  
467 improvements in the measurement of the parameters we use in this analysis would likely improve  
468 the desired end result – the prediction of the Lake Chad surface area in time to be used for  
469 agricultural decisions.

470

#### 471 **Acknowledgements**

472 Support for this research was provided by the NASA Goddard Space Flight Center's  
473 Academic Investment for Mission Success (AIMS) Program. Support for this research was also  
474 provided by NASA under its Research Opportunities in Space and Earth Sciences (ROSES)-2013  
475 Interdisciplinary Studies (IDS) Program (solicitation NNH13ZDA001N-IDS) through the  
476 Radiation Sciences Program. We appreciate the efforts of providers of the data products used for  
477 this study from various satellite sensors and models, particularly lake imagery from USGS, lake  
478 height data from USDA, CHIRPS precipitation data from U.C. Santa Barbara, evapotranspiration  
479 data from the FEWS NET Land Data Assimilation System (FLDAS), the southern Lake Chad  
480 Basin shapefile from WWF, meteorological data from NOAA NCEP-DOE, and Lake Chad  
481 surface water area from (Leblanc et al., 2011).

482

483 **Role of the funding Sources:** The funding sources had no role in the study design; in the  
484 collection, analysis and interpretation of data; in the writing of the report; or in the decision to  
485 submit the article for publication.

486

487 **Author Contributions:** Frederick Policelli and Ben Zaitchik conceived and designed the  
488 experiments; Frederick Policelli and Alfred Hubbard performed the experiments; Frederick Policelli,  
489 Hahn Chul Jung, and Ben Zaitchik analyzed the data; Charles Ichoku helped conceive the  
490 experiments and provided domain knowledge; Frederick Policelli wrote the paper with contributions  
491 from all co-authors.

492

493 **Declarations of Interest:** None

494

#### 495 **References**

496 Austin, P.C., Steyerberg, E.W., 2015. The number of subjects per variable required in linear  
497 regression analyses. *J. Clin. Epidemiol.* 68, 627–636.

498 <https://doi.org/10.1016/j.jclinepi.2014.12.014>

499

500 Bader, J.-C., Lemoalle, J., Leblanc, M., 2011. Modèle hydrologique du lac Tchad. *Hydrol. Sci.*  
501 *Journal–Journal Sci. Hydrol.* 56, 411–425.

502

503 Badr, H.S., Dezfuli, A.K., Zaitchik, B.F., Peters-Lidard, C.D., 2016. Regionalizing Africa:  
504 Patterns of Precipitation Variability in Observations and Global Climate Models. *J. Clim.*  
505 29, 9027–9043. <https://doi.org/10.1175/JCLI-D-16-0182.1>

506

507 Birkett, C.M., 2000. Synergistic remote sensing of Lake Chad: Variability of basin inundation.



508 Remote Sens. Environ. 72, 218–236.

509

510 Busker, T., de Roo, A., Gelati, E., Schwatke, C., Adamovic, M., Bisselink, B., Pekel, J.-F.,  
511 Cottam, A., 2018. A global lake and reservoir volume analysis using a surface water dataset and  
512 satellite altimetry. *Hydrol. Earth Syst. Sci. Discuss.* 1–32. <https://doi.org/10.5194/hess-2018-21>

513

514 Carmouze, J.-P., Durant, J.R., Lévêque, C., 1983. *Lake Chad: ecology and productivity of a*  
515 *shallow tropical ecosystem.* Springer Science & Business Media.

516

517 Coe, M.T., Birkett, C.M., 2004. Calculation of river discharge and prediction of lake height from  
518 satellite radar altimetry: Example for the Lake Chad basin. *Water Resour. Res.* 40,  
519 W10205. <https://doi.org/10.1029/2003WR002543>

520

521 Coe, M.T., Foley, J.A., 2001. Human and natural impacts on the water resources of the Lake  
522 Chad basin. *J. Geophys. Res. Atmospheres* 106, 3349–3356.  
523 <https://doi.org/10.1029/2000JD900587>

524

525 Delclaux, F., Le Coz, M., Coe, M., Favreau, G., Ngounou Gatcha, B., 2008. Confronting models  
526 with observations for evaluating hydrological change in the lake chad basin, Africa, in:  
527 XIIIth World Water Congress. URL:  
528 [https://www.iwra.org/member/congress/resource/abs355\\_article.pdf](https://www.iwra.org/member/congress/resource/abs355_article.pdf) accessed 7/18/2018

529

530 Funk, C., Peterson, P., Landsfeld, M., Pedreros, D., Verdin, J., Shukla, S., Husak, G., Rowland,  
531 J., Harrison, L., Hoell, A., Michaelsen, J., 2015. The climate hazards infrared precipitation with  
532 stations—a new environmental record for monitoring extremes. *Sci. Data* 2, sdata201566.  
533 <https://doi.org/10.1038/sdata.2015.66>

534

535 Gao, H., Bohn, T.J., Podest, E., McDonald, K.C., Lettenmaier, D.P., 2011. On the causes of the  
536 shrinking of Lake Chad. *Environ. Res. Lett.* 6, 034021.

537

538 Grove, A.T., 1996. African river discharges and lake levels in the twentieth century. *Limnol.*  
539 *Climatol. Paleoclimatology East Afr. Lakes Gordon Breach Neth.* 95–100.

540

541 Harrell, F.E., Lee, K.L., Mark, D.B., 1996 Multivariable Prognostic Models: Issues in  
542 Developing Models, Evaluating Assumptions and Adequacy, and Measuring and  
543 Reducing Errors. *Stat. Med.* 15, 361–387. [https://doi.org/10.1002/\(SICI\)1097-](https://doi.org/10.1002/(SICI)1097-0258(19960229)15:4<361::AID-SIM168>3.0.CO;2-4)  
544 [0258\(19960229\)15:4<361::AID-SIM168>3.0.CO;2-4](https://doi.org/10.1002/(SICI)1097-0258(19960229)15:4<361::AID-SIM168>3.0.CO;2-4)

545

546 Lake Chad flooded savanna", World Wildlife Fund, no date,  
547 <https://www.worldwildlife.org/ecoregions/at0904> accessed 7/18/2018

548

549 Leblanc, M., Lemoalle, J., Bader, J.-C., Tweed, S., Mofor, L., 2011. Thermal remote sensing of

550 water under flooded vegetation: New observations of inundation patterns for the ‘Small’  
551 Lake Chad. *J. Hydrol.* 404, 87–98. <https://doi.org/10.1016/j.jhydrol.2011.04.023>  
552  
553 Lehner, B., Grill G., 2013. Global river hydrography and network routing: baseline data and new  
554 approaches to study the world's large river systems. *Hydrological Processes*, 27(15):  
555 2171-2186.  
556  
557 Lehner, B., Verdin, K., Jarvis, A., 2011 New Global Hydrography Derived From Spaceborne  
558 Elevation Data. *Eos Trans. Am. Geophys. Union* 89, 93–94.  
559 <https://doi.org/10.1029/2008EO100001>  
560  
561 Lemoalle, J., 2004. Lake Chad: A Changing Environment. In: Nihoul J.C.J., Zavialov P.O.,  
562 Micklin P.P. (eds) *Dying and Dead Seas Climatic Versus Anthropic Causes*. NATO  
563 Science Series: IV: Earth and Environmental Sciences, vol 36. Springer, Dordrecht  
564  
565 Lemoalle, J., Bader, J.-C., Leblanc, M., Sedick, A., 2012. Recent changes in Lake Chad:  
566 Observations, simulations and management options (1973–2011). *Glob. Planet. Change*  
567 80, 247–254.  
568  
569 McNally, A., Arsenault, K., Kumar, S., Shukla, S., Peterson, P., Wang, S., Funk, C., Peters-  
570 Lidard, C.D., Verdin, J.P., 2017. A land data assimilation system for sub-Saharan Africa food

571 and water security applications. *Sci. Data* 4, 170012. <https://doi.org/10.1038/sdata.2017.12>

572

573 Morton, F.I., 1986. Practical Estimates of Lake Evaporation. *J. Clim. Appl. Meteorol.* 25, 371–

574 387. [https://doi.org/10.1175/1520-0450\(1986\)025<0371:PEOLE>2.0.CO;2](https://doi.org/10.1175/1520-0450(1986)025<0371:PEOLE>2.0.CO;2)

575

576 Okpara, U.T., Stringer, L.C., Dougill, A.J., 2016. Lake drying and livelihood dynamics in Lake

577 Chad: Unravelling the mechanisms, contexts and responses. *Ambio* 45, 781–795.

578 <https://doi.org/10.1007/s13280-016-0805-6>

579

580 Policelli, F., Hubbard, A., Jung, H.C., Zaitchik, B., Ichoku, C., 2018. Lake Chad Total Surface

581 Water Area as Derived from Land Surface Temperature and Radar Remote Sensing Data.

582 *Remote Sens.* 10, 252. <https://doi.org/10.3390/rs10020252>

583

584 Ricko, M., Carton, J.A., Birkett, C.M., Cretaux, J.-F., 2012. Intercomparison and validation of

585 continental water level products derived from satellite radar altimetry. *J. Appl. Remote*

586 *Sens.* 6, 061710. <https://doi.org/10.1117/1.JRS.6.061710>

587

588 Sarch, M.-T., Birkett, C., 2000. Fishing and farming at Lake Chad: Responses to lake-level

589 fluctuations. *Geogr. J.* 166, 156–172.

590

591 Satellite Radar Altimetry: Global Reservoir and Lake Elevation Database [WWW Document], no

592 date URL [https://www.pecad.fas.usda.gov/cropexplorer/global\\_reservoir/](https://www.pecad.fas.usda.gov/cropexplorer/global_reservoir/) (accessed

593 10.17.17).

594  
595 Schneider, Udo; Becker, Andreas; Finger, Peter; Meyer-Christoffer, Anja; Rudolf, Bruno; Ziese,  
596 Markus (2015): GPCC Full Data Monthly Product Version 7.0 at 0.5<sup>0</sup> : Monthly Land-  
597 Surface Precipitation from Rain-Gauges built on GTS-based and Historic Data. DOI:  
598 10.5676/DWD GPCC/FD M V7 050

599  
600 Senay, G.B., Bohms, S., Singh, R.K., Gowda, P.H., Velpuri, N.M., Alemu, H., Verdin, J.P., 2013  
601 Operational Evapotranspiration Mapping Using Remote Sensing and Weather Datasets:  
602 A New Parameterization for the SSEB Approach. JAWRA J. Am. Water Resour. Assoc.  
603 49, 577–591. <https://doi.org/10.1111/jawr.12057>

604  
605 Zhu, W., Yan, J., Jia, S., 2017a. Monitoring Recent Fluctuations of the Southern Pool of Lake  
606 Chad Using Multiple Remote Sensing Data: Implications for Water Balance Analysis.  
607 Remote Sens. 9, 1032. <https://doi.org/10.3390/rs9101032>

608

## 609 **Appendix**

610 We examined the correlation between P–ET for the southern Lake Chad Basin and the lake  
611 elevation variation relative to 1993-2002 for 1992 to 2017, and found the maximum correlation  
612 of 0.69 at four months lag time between these variables. Next, we examined the correlation  
613 between the P–ET for the southern part of the basin and the lake surface area and found the  
614 maximum correlation of 0.37 at eight months lag time. We also examined the correlation

615 between the lake elevation variation and the lake surface water area and found the maximum  
616 correlation of 0.57 at four months lag time. We found a maximum correlation of 0.43 for ET vs  
617 the lake's surface water area at 7 months, and a correlation of 0.63 for the surface water area  
618 versus the previous year's surface water area for the same month. There is apparently memory  
619 of the previous year's area in the system.

620 To determine the value added by the ET data to our analysis, we examined the correlation  
621 between precipitation (without subtracting ET) for the southern Lake Chad Basin and the lake  
622 elevation and found an increase in the maximum correlation to 0.80 at four months lag time. We  
623 found the correlation between the percentage of the 1988-2016 average lake ET and the lake total  
624 surface water area to be 0.65 at zero lag time. We also examined the correlation between  
625 precipitation and total lake surface area and found an increase in the maximum correlation to  
626 0.39 at seven months lag time. This is the same lag time as for the maximum correlation  
627 between ET and total lake surface area and represents the time it takes for much of the net  
628 precipitation to make its way from run off in the southernmost part of the Lake Chad basin, to  
629 flowing through the Chari-Logone River system, to reaching the lake and causing an increase in  
630 the lake area. A surprising result of the correlation analysis is that the use of FLDAS ET data in  
631 the analysis to produce (P-ET) causes a small decrease in the correlation numbers relative to  
632 what is achieved with precipitation alone. Note however that ET is somewhat more closely  
633 correlated with total lake surface water area than is precipitation (.43 vs. .39, both at 7 months lag  
634 time). Precipitation and ET have a maximum correlation coefficient of 0.93 with a one month  
635 delay between the two.